Available online at www.sciencedirect.com
SCIENCE DIRECT®
International Journal of Solids and Structures 42 (2005) 5491–5512
INTERNATIONAL JOURNAL OF SOLIDS and STRUCTURES
www.elsevier.com/locate/ijsolstr

Interacting elliptic inclusions by the method of complex potentials

V.I. Kushch [a,*], S.V. Shmegera [a], V.A. Buryachenko [b]

[a] *Institute for Superhard Materials of the National Academy of Sciences, 04074 Kiev, Ukraine*
[b] *University of Dayton Research Institute, Dayton, OH 45469-0168, USA*

Received 6 October 2004; received in revised form 19 February 2005
Available online 18 April 2005

Abstract

An accurate series solution has been obtained for a piece-homogeneous elastic plane containing a finite array of non-overlapping elliptic inclusions of arbitrary size, aspect ratio, location and elastic properties. The method combines standard Muskhelishvili's representation of general solution in terms of complex potentials with the superposition principle and newly derived re-expansion formulae to obtain a complete solution of the many-inclusion problem. By exact satisfaction of all the interface conditions, a primary boundary-value problem stated on a complicated heterogeneous domain has been reduced to an ordinary well-posed set of linear algebraic equations. A properly chosen form of potentials provides a remarkably simple form of solution and thus an efficient computational algorithm. The theory developed is rather general and can be applied to solve a variety of composite mechanics problems. The advanced models of composite involving up to several hundred inclusions and providing an accurate account for the microstructure statistics and fiber–fiber interactions can be considered in this way. The numerical examples are given showing high accuracy and numerical efficiency of the method developed and disclosing the way and extent to which the selected structural parameters influence the stress concentration at the matrix–inclusion interface.

Keywords: Linear elasticity; Elliptic inclusions; Complex potentials; Local expansion; Stress concentration; Stress intensity factor

1. Introduction

The method of complex potentials developed more than 50 years ago by Muskhelishvili (1953) is now well recognized as a powerful and easy-to-use tool for solving a variety of two-dimensional (2D) linear

* Corresponding author. Tel./fax: +380 444329544.
E-mail address: vkushch@bigmir.net (V.I. Kushch).

0020-7683/$ - see front matter © 2005 Elsevier Ltd. All rights reserved.
doi:10.1016/j.ijsolstr.2005.02.035

elasticity problems including those stated on the multiply connected domains. This fact makes the method attractive and potentially very useful in micromechanics of fibrous composites because it provides an efficient tool for analyzing the advanced many-inclusion model problems with an accurate account for the fiber–fiber interaction. In the theoretical study of composites reinforced by unidirectional circular fibers, the method has been applied successfully by Horii and Nemat-Nasser (1985), Golovchan et al. (1993), Buryachenko and Kushch (in press), among many others.

At the same time, to the best of the authors' knowledge, the works where interaction of elliptic in cross-section fibers were studied by the method of complex potentials are absent. Moreover, we could not find in the literature a solution of even a single elliptic inclusion problem being a particular limiting case of well-known Eshelby's solution, written in terms of complex potentials. This fact, at first sight, is somewhat surprising because the solution of a similar problem, namely, an elastic plane with several holes of general shape, can be found in a regular textbook on the theory of analytical functions. The matter here is that the conformal mapping technique working so perfectly for a plane with holes does not allow straightforward extension on the case of inhomogeneities.

To study interaction between the elliptic inclusions, both the numerical and analytical methods were applied. Among the works based on numerical analysis, we mention Bystroem (2003) who combined the cell model approach with the finite element method to evaluate effective stiffness of a composite of long elliptic fibers. To study interaction of two elliptic inclusions, the method of singular integral equations was utilized by Noda and Matsumo (1998). As to analytical solutions, here, probably, the most comprehensive work was done by Meisner and Kouris (1995). To obtain a series solution for two identical, symmetrically placed elliptic inhomogeneities embedded in an infinite plane, they made use of the Papkovich-Neihber representation of general solution in terms of real potentials. Derived by accurate matching of the elastic fields in the matrix and inclusions an infinite set of equations appears, however, to be rather involved and thus difficult to use; also, it is uncertain whether or not it possible to extend the solution obtained in this way on more general geometry of problem.

It was mentioned already that using the complex potentials in 2D linear elasticity is advantageous and much more fruitful in comparison with their real-valued counterparts. At the same time, the common knowledge is that the method of potentials is efficient only where the potential functions were taken in the proper form.[1] Several attempts had been made to apply the theory of complex potentials to solve for interaction between the elliptic inclusions, but up to now, only partial solutions were found. So, the point-to-point collocation scheme has been utilized by Kosmodamiansky (1972) to fulfill the matrix–inclusion interface bonding conditions; Kaloerov and Goryanskaya (1995) have applied the least square fitting to determine the unknown series expansion coefficients. Both the approaches, strictly speaking, cannot be regarded as rigorous from a mathematical standpoint; not surprisingly, the corresponding numerical algorithms appeared to be rather unstable (see, e.g., Lu and Kim, 1990).

In the present work, an accurate series solution has been developed for an elastic plane containing a finite array of non-overlapping elliptic inhomogeneities. We impose no restrictions on their number, size, aspect ratio, elastic properties and arrangement. The only condition adopted here for simplicity sake is that all the inclusions are equally oriented; however, with minor modifications, this approach is able to study arbitrarily oriented inclusions as well. In what follows, the basic notations are introduced first and a general solution has been obtained for a single elliptic inclusion in an elastic plane subject to inhomogeneous external stress field. Then, this solution has been combined with the superposition principle and re-expansion formulae to derive a complete solution of the many-inclusion problem. In Section 4, application of the the-

[1] It is appropriate to mention here the work by Stevenson (1942) who suggested a special form of complex potentials in the single elliptic hole problem and obtained the solution in a much more simple and elegant way as compared with the standard conformal mapping technique.

ory developed to the composite micromechanics problems is discussed. The results of the numerical study are summarized in the last section and, finally, two appendices provide all the necessary background theory.

2. Single elliptic inclusion in an inhomogeneous external field

Consider an infinite isotropic elastic solid with a single, elliptic in cross-section, long fiber embedded. We assume the external load to be applied in a way that the stress field does not vary in the fiber axis direction. In this case, the problem can be stated as 2D (plane strain or plane stress formulation), which, in turn, enables using the method of complex potentials. To describe geometry of the problem, we introduce first the Cartesian coordinate system Ox_1x_2 so that its origin coincides with the centroid of ellipse whereas the Ox_1 and Ox_2 axes are directed along the major and minor axes of the ellipse. An aspect ratio of the ellipse is $e = l_2/l_1$, where l_1 and l_2 are the major and minor, respectively, semi-axes of the ellipse. Another derivative geometric parameter to be used in subsequent analysis is the inter-foci distance $2d$, where $d = \sqrt{l_1^2 - l_2^2}$.

We also introduce two kinds of complex variables. The first one is a point of Cartesian complex plane $z = x_1 + \mathrm{i}x_2$. The second variable $\xi = \zeta + \mathrm{i}\eta$ is defined as

$$z = \omega(\xi) = d\cosh\xi. \tag{1}$$

Eq. (1) defines, in fact, an elliptic coordinate system with ζ and η as "radial" and "angular" coordinates, respectively. So, the boundary of the ellipse is the coordinate line given by the equation

$$\zeta = \zeta_0 = \ln\left(\frac{l_1 + l_2}{d}\right) = \frac{1}{2}\ln\left(\frac{1+e}{1-e}\right), \tag{2}$$

i.e., the points at matrix–elliptic fiber interface are the functions of angular coordinate η only. This fact makes the elliptic complex variable ξ particularly useful in the problems formulated on domains with elliptic boundaries/interfaces.

Following Muskhelishvili (1953), we express the displacement vector $\mathbf{u} = (u_1, u_2)^{\mathrm{T}}$ in terms of complex potentials φ and ψ, namely

$$u = u_1 + \mathrm{i}u_2 = \varkappa\varphi(z) - (z - \bar{z})\overline{\varphi'(z)} - \overline{\psi(z)}, \tag{3}$$

where $\varkappa = 3 - 4\nu$ for plane strain and $\varkappa = \frac{3-\nu}{1+\nu}$ for plane stress problem; ν is Poisson's ratio and $\bar{z}$ means complex conjugate of z. Noteworthy, the expression (3) is slightly different in form but equivalent to formulas originally suggested by Muskhelishvili. In fact, (3) reduces to the standard form by replacing $\psi(z)$ with $\psi(z) - z\varphi'(z)$, the latter being an analytical function of variable z as well. However, as will be shown below, representation (3) is advantageous for our purpose in several aspects. Corresponding to $\mathbf{u}$ (3) the Cartesian components of stress tensor $\boldsymbol{\sigma}$ are given by

$$\sigma_{11} + \sigma_{22} = 4G\left(\varphi'(z) + \overline{\varphi'(z)}\right), \tag{4}$$

$$\sigma_{22} - \sigma_{11} + 2\mathrm{i}\sigma_{12} = 4G[(\bar{z} - z)\varphi''(z) - \varphi'(z) + \psi'(z)],$$

where G is a shear modulus, $\boldsymbol{\sigma} = \mathbf{L}\boldsymbol{\varepsilon}$ and $\boldsymbol{\varepsilon} = \frac{1}{2}[\nabla\mathbf{u} + (\nabla\mathbf{u})^{\mathrm{T}}]$.

The displacement $\mathbf{u}$ and traction $\mathbf{T}_n = \boldsymbol{\sigma}\cdot\mathbf{n}$ are assumed to be continuous through the elliptic matrix–inclusion interface $\zeta = \zeta_0$:

$$[[\mathbf{u}]]_{\zeta=\zeta_0} = 0, \quad [[\boldsymbol{\sigma}\cdot\mathbf{n}]]_{\zeta=\zeta_0} = 0, \tag{5}$$

where $[[\mathbf{f}]]_S$ means a jump of $\mathbf{f}$ through the boundary S: so, $[[\mathbf{u}]]_{\zeta=\zeta_0} = (\mathbf{u}^{(0)} - \mathbf{u}^{(1)})_{\zeta=\zeta_0}$ and upper indices "0" and "1" refer to matrix and inclusion, respectively. Also, $G = G_0$, $\nu = \nu_0$ in the matrix and $G = G_1$, $\nu = \nu_1$ in

the inclusion. Satisfying the conditions (5) can be greatly simplified by re-writing displacement and traction vectors in (5) in terms of their curvilinear (actually, normal and tangential to interface $\zeta = \zeta_0$) components:

$$u = u_\zeta + \mathrm{i}u_\eta \quad \text{and} \quad T_n = \sigma_{\zeta\zeta} + \mathrm{i}\sigma_{\zeta\eta}. \tag{6}$$

They also can be expressed in terms of complex potentials (Muskhelishvili, 1953):

$$u_\zeta + \mathrm{i}u_\eta = \frac{\overline{\omega'(\xi)}}{|\omega'(\xi)|}[\varkappa\varphi(z) - (z-\bar{z})\overline{\varphi'(z)} - \overline{\psi(z)}], \tag{7}$$

$$\sigma_{\zeta\zeta} - \mathrm{i}\sigma_{\zeta\eta} = 2G\left\{\varphi'(z) + \overline{\varphi'(z)} - \frac{\omega'(\xi)}{\overline{\omega'(\xi)}}[(\bar{z}-z)\varphi''(z) - \varphi'(z) + \psi'(z)]\right\},$$

where, from (1), $\omega'(\xi) = \mathrm{d}z/\mathrm{d}\xi = d\sinh\xi$.

The key point is, of course, the proper choice of the form of potential functions φ and ψ. A simple and straightforward (but, definitely, not the best) way is to write them by analogy with Meisner and Kouris (1995) for, say, matrix domain V_0 as

$$\varphi = \sum_n A_n \upsilon^{-n}, \quad \psi = \sum_n B_n \upsilon^{-n}, \tag{8}$$

where A_n and B_n are the complex-valued coefficients, and $\upsilon = \exp\xi$. However, in this case the resolving set of equations appears to be rather complicated and, moreover, the Eshelby-type problem known to possess exact closed form solution is given by infinite series. We take ψ, by analogy to the 3D case (Kushch, 1996), in the following form:

$$\psi = \psi_0 - \psi_1, \quad \psi_0 = \sum_n B_n \upsilon^{-n}, \quad \psi_1 = \frac{\sinh\zeta_0}{\sinh\xi}\left(\frac{\upsilon}{\upsilon_0} - \frac{\upsilon_0}{\upsilon}\right)\sum_n nA_n\upsilon^{-n}, \tag{9}$$

where $\upsilon_0 = \exp(\zeta_0)$. As is obvious, (9) is an analytical function of z; indeed, the functions $\frac{\upsilon^n}{\sinh\xi} = \frac{d}{n}\frac{\mathrm{d}\upsilon^n}{\mathrm{d}z}$ can be considered as an alternate set of basis functions in (8) obtained by differentiation of υ^n with respect to z. The potentials φ_i and ψ_i for solution in the inclusion V_1 are also given by (8) and (9), with replacing A_n and B_n to C_n and D_n, respectively; C_n and D_n are also the complex-valued coefficients, which, as well as A_n and B_n, are found from the interface condition (5).

With φ in the form (8) and ψ in the form (9), the expression of u and T_n (7) at the interface $\zeta = \zeta_0$ is simplified dramatically; for details of derivation, see Appendix A. So, by virtue of (A.5), from the first condition (5) one finds $[[u]]_{\zeta=\zeta_0} = [[\varkappa\varphi - \overline{\psi_0}]]_{\zeta=\zeta_0} = 0$; in explicit form,

$$\sum_n(\varkappa_0 A_n \mathrm{e}^{-n\zeta_0 - \mathrm{i}n\eta} - \overline{B}_n \mathrm{e}^{-n\zeta_0 + \mathrm{i}n\eta}) = \sum_n(\varkappa_1 C_n \mathrm{e}^{-n\zeta_0 - \mathrm{i}n\eta} - \overline{D}_n \mathrm{e}^{-n\zeta_0 + \mathrm{i}n\eta}), \tag{10}$$

where $\varkappa_i = \varkappa(\nu_i)$. Using the orthogonality property of Fourier harmonics $\exp(\mathrm{i}n\eta)$ reduces the functional equality (10) to an infinite set of linear algebraic equations

$$\varkappa_0 A_n \upsilon_0^{-n} - \overline{B}_{-n}\upsilon_0^n = \varkappa_1 C_n \upsilon_0^{-n} - \overline{D}_{-n}\upsilon_0^n. \tag{11}$$

By applying the same procedure to the second condition in (5) and taking account of (A.13) re-written as $[[\omega' T_n]]_{\zeta=\zeta_0} = [[2G(\varphi' - \overline{\psi_0'})]]_{\zeta=\zeta_0} = 0$ we get another set of linear equations:

$$A_n\upsilon_0^{-n} + \overline{B}_{-n}\upsilon_0^n = \lambda(C_n\upsilon_0^{-n} + \overline{D}_{-n}\upsilon_0^n), \tag{12}$$

where $\lambda = G_1/G_0$.

It is advisable, for computational purpose, to introduce new scaled variables $\widetilde{A}_n = A_n\upsilon_0^{-n}$, etc.; we obtain

$$\varkappa_0\widetilde{A}_n - \overline{\widetilde{B}}_{-n} = \varkappa_1\widetilde{C}_n - \overline{\widetilde{D}}_{-n}, \tag{13}$$

$$\widetilde{A}_n + \overline{\widetilde{B}}_{-n} = \lambda(\widetilde{C}_n + \overline{\widetilde{D}}_{-n}), \quad -\infty < n < \infty.$$

The form of Eq. (13) is remarkably simple, if not simplest (see, for comparison, Meisner and Kouris (1995)) which clearly indicates rational choice of the potential functions (9).

The solution we derived is rather general and in each specific case, the extra degrees of freedom can be excluded by imposing certain additional constraints drawn from physical considerations. One of them is the regularity condition of the displacement field inside the inclusion; i.e., it must be continuous and finite for $z \in V_1$ meaning that Laurent series expansions of corresponding complex potentials contain the terms with non-negative powers of z only. It has been shown in Appendix A that the following relations between C_n and D_n with positive and negative index n,

$$C_n = C_{-n}, \quad D_n = D_{-n} + 2n\sinh(2\zeta_0)C_{-n}, \quad n > 0, \tag{14}$$

provide regularity of $u^{(1)}$ and $\sigma^{(1)}$ inside the inclusion.

As to solution in the matrix domain, it is natural to represent it as a sum of regular and singular parts, $u^{(0)} = u^r + u^s$. Here, u^r is the incident, or far field, whereas u^s describes disturbance field induced by the inclusion; expectably, $u^s \to 0$ as $|z| \to \infty$. The corresponding potentials φ and ψ also can be divided onto singular and regular parts

$$\varphi = \varphi^s + \varphi^r, \quad \psi = \psi^s + \psi^r. \tag{15}$$

The explicit form of φ^s and ψ^s is given by Eqs. (8) and (9), respectively, where we keep the terms with negative powers of υonly to provide vanishing of disturbance field at infinity, so

$$A_n = B_n \equiv 0 \quad \text{for } n \leqslant 0. \tag{16}$$

On the contrary, u^r is assumed to be regular, with the potentials

$$\varphi^r = \sum_n a_n \upsilon^{-n}, \quad \psi^r = \sum_n \left[b_n - 2na_n \frac{\sinh\zeta_0}{\sinh\xi}\sinh(\xi - \zeta_0) \right] \upsilon^{-n}, \tag{17}$$

where a_n and b_n comply (14) as well. For example, let us consider a far field induced by the remote constant strain tensor $\boldsymbol{\varepsilon}_\infty = \{E_{ij}\}$. Representation of the corresponding linear displacement field

$$u^r = (E_{11}x_1 + E_{12}x_2) + \mathrm{i}(E_{12}x_1 + E_{22}x_2), \tag{18}$$

takes the form (3) with the potentials (17), where

$$a_{-1} = \frac{d}{4}\frac{E_{11} + E_{22}}{(\varkappa_0 - 1)}, \quad b_{-1} = a_{-1}\upsilon_0^{-2} + \frac{d}{4}(E_{22} - E_{11} + 2\mathrm{i}E_{12}), \tag{19}$$

a_1 and b_1 are given by (14) and all other a_n and b_n for $n \neq \pm 1$ are equal to zero. For the far stress tensor $\boldsymbol{\sigma}_\infty = \{S_{ij}\}$ instead of $\boldsymbol{\varepsilon}_\infty$ prescribed, we have quite similar expressions:

$$a_{-1} = \frac{d}{16G_0}(S_{11} + S_{22}), \quad b_{-1} = a_{-1}\upsilon_0^{-2} + \frac{d}{8G_0}(S_{22} - S_{11} + 2\mathrm{i}S_{12}). \tag{20}$$

The displacement u^r and corresponding traction T_n^r at the interface $\zeta = \zeta_0$ take the form (A.5) and (A.13), respectively. Applying the procedure analogous to that described above gives us an infinite linear system

$$\varkappa_0 A_n \upsilon_0^{-n} - \overline{B}_{-n}\upsilon_0^n + \varkappa_0 a_n \upsilon_0^{-n} - \overline{b}_{-n}\upsilon_0^n = \varkappa_1 C_n \upsilon_0^{-n} - \overline{D}_{-n}\upsilon_0^n, \tag{21}$$

$$A_n\upsilon_0^{-n} + \overline{B}_{-n}\upsilon_0^n + a_n\upsilon_0^{-n} + \overline{b}_{-n}\upsilon_0^n = \lambda(C_n\upsilon_0^{-n} + \overline{D}_{-n}\upsilon_0^n).$$

In the one-inclusion problem considered in this section, we assume u^r (or, the same, a_n and b_n) to be known. In this case, Eq. (21) together with (14) and (16) form a closed set of linear algebraic equations possessing a unique solution. By substituting (14) and (16) into (21) we come to resolving system

$$\begin{aligned}
&\varkappa_0 A_n - \varkappa_1 C_n + (\overline{D}_n - 2n\sinh 2\zeta_0 \overline{C}_n)\upsilon_0^{2n} = -\varkappa_0 a_n + \overline{b}_{-n}\upsilon_0^{2n},\\
&\overline{B}_n + \varkappa_1 C_n \upsilon_0^{2n} - \overline{D}_n = \varkappa_0 a_{-n}\upsilon_0^{2n} - \overline{b}_n,\\
&A_n - \lambda C_n - \lambda(\overline{D}_n - 2n\sinh 2\zeta_0 \overline{C}_n)\upsilon_0^{2n} = -a_n - \overline{b}_{-n}\upsilon_0^{2n},\\
&\overline{B}_n - \lambda C_n \upsilon_0^{2n} - \lambda \overline{D}_n = -a_{-n}\upsilon_0^{2n} - \overline{b}_n, \quad n = 1, 2, \ldots,
\end{aligned} \tag{22}$$

with the unknowns A_n, B_n, C_n and D_n ($n > 0$) and with the coefficients a_n and b_n entering the right-hand side vector. For the Eshelby-type problem with the constant far strain $\boldsymbol{\varepsilon}_\infty$ or stress field $\boldsymbol{\sigma}_\infty$ is prescribed, these coefficients are given by (19) or (20), respectively. The corresponding resolving system (22) consists of four equations for $n = 1$; for the explicit expressions of the coefficients A_1, B_1, C_1 and D_1, see Section 4, Eq. (56).

The solution we derived is valid for any $0 < e < 1$. To complete this section, we consider the limiting case $e \to 0$ where the ellipse degenerates into the cut $|x_1| \leqslant d$ in the complex plane (another limit, $e \to 1$ when the ellipse becomes a circle is rather trivial). By putting $\lambda = 0$ we get a straight crack, the stress field around which is known to have singularity in the crack tips. In the linear fracture mechanics, the parameter called stress intensity factor (SIF) and defined as

$$K_\mathrm{I} + \mathrm{i}K_\mathrm{II} = \lim_{z\to d} \sqrt{2\pi(z-d)}(\sigma_{22} + \mathrm{i}\sigma_{12}) \tag{23}$$

is generally accepted to quantify the stress field near the tip of crack. No problems arise with taking this limit in the above solution: for $e \to 0$ we have, from (2), $\zeta_0 \to 0$ and $\upsilon_0 \to 1$. After some standard algebra one obtains the formula

$$K_\mathrm{I} + \mathrm{i}K_\mathrm{II} = -2G_0\sqrt{\pi/d}\sum_{n=1}^{\infty} n\left(A_n + \overline{B}_n\right), \tag{24}$$

valid for arbitrary, not necessarily uniform, external load.

3. Finite array of inclusions

Now, we proceed with a piece-homogeneous plane containing a finite number N of non-overlapping elliptic inclusions V_p with semi-axes l_{1p}, l_{2p} and elastic moduli G_p and ν_p, $p = 1, 2, \ldots, N$. The centroid of the pth ellipse lies in the point $Z_p = X_{1p} + \mathrm{i}X_{2p}$; for simplicity sake, we assume all ellipses to be equally oriented. Also, we introduce local Cartesian coordinate systems $O_p x_{1p} x_{2p}$ centered in Z_p. The local coordinates of different systems are related by

$$z_p = Z_{pq} + z_q, \quad \text{where } z_p = x_{1p} + \mathrm{i}x_{2p} \text{ and } Z_{pq} = Z_q - Z_p. \tag{25}$$

Next, we define the local curvilinear coordinates $\xi_p = \zeta_p + \mathrm{i}\eta_p$ by analogy with (1): $z_p = d_p \cosh \xi_p$. In these variables, the geometry of the pth inclusion can be alternatively defined by a pair of parameters (ξ_{0p}, d_p), where $d_p = \sqrt{(l_{1p})^2 - (l_{2p})^2}$. At the matrix–inclusion interface $\xi_p = \xi_{0p}$, the perfect bonding

$$[[\mathbf{u}]]_{\zeta_p=\zeta_{0p}} = 0, \quad [[\boldsymbol{\sigma}\cdot\mathbf{n}]]_{\zeta_p=\zeta_{0p}} = 0, \quad p = 1, 2, \ldots, N, \tag{26}$$

is assumed. The stress in and around the inclusions is induced by the far field u^r: we assume it in the form (18).

To write the solution for a multiply connected matrix domain, owing to linearity of the problem, we make use of the superposition principle:

$$u^{(0)} = u^r(z) + \sum_{p=1}^{N} u_p^s(z - Z_p), \tag{27}$$

where u_p^s is a disturbance induced by the pth inclusion and decaying at $|z| \to \infty$. The corresponding complex potentials φ_p^s and ψ_p^s are again taken in the form (8) and (9), where, by analogy with (16), $A_{np} = B_{np} = 0$ for $n \leqslant 0$.

Note that the separate terms of sum in (27) are written in variables of different coordinate systems. Therefore, in order to satisfy the interface conditions (26) for, say qth inclusion in a way exposed in the previous section, we need to find local expansion of (27), i.e., express all its terms in variables of a given local coordinate system. Our aim is to transform

$$u_p^s = \varkappa_0 \varphi_p^s(z_p) - (z_p - \bar{z}_p)\overline{\varphi_p^{s'}(z_p)} - \overline{\psi_p^s(z_p)}, \tag{28}$$

where

$$\varphi_p^s = \sum_{n=0}^{\infty} A_{np} \upsilon_p^{-n}, \tag{29}$$

$$\psi_p^s = \psi_{0p}^s - \psi_{1p}^s = \sum_{n=0}^{\infty} \left[B_{np} - 2nA_{np} \frac{\sinh \zeta_{0p}}{\sinh \xi_p} \sinh(\xi_p - \zeta_{0p}) \right] \upsilon_p^{-n},$$

into u_{pq}^r, written in the same form as u_p^s, but in the qth coordinate basis, namely

$$u_{pq}^r = \varkappa_0 \varphi_{pq}^r(z_q) - (z_q - \bar{z}_q)\overline{\varphi_{pq}^{r'}(z_q)} - \overline{\psi_{pq}^r(z_q)}, \tag{30}$$

with

$$\varphi_{pq}^r = \sum_n a_{npq} \upsilon_q^{-n}, \tag{31}$$

$$\psi_{pq}^r = \psi_{0pq}^r - \psi_{1pq}^r = \sum_n \left[b_{npq} - 2na_{npq} \frac{\sinh \zeta_{0q}}{\sinh \xi_q} \sinh(\xi_q - \zeta_{0q}) \right] \upsilon_q^{-n}.$$

For this purpose, we utilize the re-expansion formulas (referred sometimes as the addition theorems) for the complex potentials, derived in Appendix B. So, by applying (B.1) to φ_p^s we obtain

$$\varphi_p^s = \sum_{n=0}^{\infty} A_{np} \upsilon_p^{-n} = \sum_n a_{npq} \upsilon_q^{-n} = \varphi_{pq}^r, \tag{32}$$

from where we immediately get

$$a_{npq} = \sum_{m=1}^{\infty} A_{mp} \eta_{mn}^{pq}, \tag{33}$$

where η_{mn}^{pq} are the re-expansion coefficients given by (B.9). With a_{npq} taken in the form (33) the first terms in (28) and (30) coincide, $\varkappa_0 \varphi_p^s = \varkappa_0 \varphi_{pq}^r$.

Determination of b_{npq} is somewhat more involved. From (32) we conclude also $\varphi_p^{s'}(z_p) = \varphi_{pq}^{r'}(z_q)$ and thus the second term in (28) can be transformed as

$$(z_p - \bar{z}_p)\varphi_p^{s'} = (Z_{pq} - \overline{Z_{pq}})\varphi_{pq}^{r'} + (z_q - \bar{z}_q)\varphi_{pq}^{r'}. \tag{34}$$

To provide $u_p^s = u_{pq}^r$, we determine b_{npq} in (31) from

$$\psi_p^s = \psi_{pq}^r + (Z_{pq} - \overline{Z_{pq}})\varphi_{pq}^{r'}. \tag{35}$$

To this end, all the terms in (35) should be expanded into a series of υ_q; below, we outline the derivation procedure.

The simplest thing is ψ^s_{0p}: likewise φ^s_p (32) and (33), we write

$$\psi^s_{0p} = \sum_{n=1}^{\infty} B_{np}\upsilon_p^{-n} = \sum_n \left(\sum_{m=1}^{\infty} B_{mp}\eta^{pq}_{mn}\right)\upsilon_q^{-n}. \tag{36}$$

Next, we re-group ψ^s_{1p} as

$$\psi^s_{1p} = \sum_{n=1}^{\infty} nA_{np}\left[\left(1-\upsilon_{0p}^{-2}\right)\upsilon_p^{-n} - \frac{1}{2}\left(\upsilon_{0p}-\upsilon_{0p}^{-1}\right)^2\frac{\upsilon_p^{-(n+1)}}{\sinh\xi_p}\right]. \tag{37}$$

With the aid of (B.1) and (B.11), ψ^s_{1p} can be expanded into

$$\psi^s_{1p} = \sum_n \left\{\sum_{m=1}^{\infty} mA_{mp}\left[\left(1-\upsilon_{0p}^{-2}\right)\eta^{pq}_{mn} - \frac{1}{2}\left(\upsilon_{0p}-\upsilon_{0p}^{-1}\right)^2\mu^{pq}_{m+1,n}\right]\right\}\upsilon_q^{-n}. \tag{38}$$

where μ^{pq}_{mn} are the re-expansion coefficients in (B.11). Similarly to (37), ψ^r_{1pq} can be re-arranged to

$$\psi^r_{1pq} = \left(1-\upsilon_{0q}^{-2}\right)\sum_n na_{npq}\upsilon_q^{-n} + \left(\upsilon_{0q}-\upsilon_{0q}^{-1}\right)^2\sum_{n=1}^{\infty} na_{npq}\frac{\upsilon_q^{n+1}-\upsilon_q^{-(n+1)}}{\upsilon_q-\upsilon_q^{-1}}, \tag{39}$$

by applying the formula

$$\frac{\upsilon^{n+1}-\upsilon^{-(n+1)}}{\upsilon-\upsilon^{-1}} = \sum_{k=0}^{n}\upsilon^{2k-n} \tag{40}$$

and (33) we get

$$\psi^r_{1pq} = \sum_n \left\{\sum_{m=1}^{\infty} A_{mp}\left[\left(\upsilon_{0q}^{-2}-1\right)|n|\eta^{pq}_{m|n|} + \left(\upsilon_{0q}-\upsilon_{0q}^{-1}\right)^2\sum_{k=0}^{\infty}(|\,n\,|+2k)\eta^{pq}_{m,|n|+2k}\right]\right\}\upsilon_q^{-n}. \tag{41}$$

The last remaining term is $(\overline{Z}_{pq}-Z_{pq})\varphi^{r'}_{pq}$; by applying to it the procedure described above, one obtains

$$\varphi^{r'}_{1pq} = \frac{2}{d_q}\sum_n \left\{\sum_{m=1}^{\infty} A_{mp}\left[\sum_{k=0}^{\infty}(|\,n\,|+1+2k)\eta^{pq}_{m,|n|+1+2k}\right]\right\}\upsilon_q^{-n}. \tag{42}$$

Collecting, finally, all the expansions gives us the following b_{npq} expression for $n<0$:

$$b_{npq} = \sum_{m=1}^{\infty} B_{mp}\eta^{pq}_{mn} + \sum_{m=1}^{\infty} A_{mp}\left\{\frac{m}{2}\left(\upsilon_{0p}-\upsilon_{0p}^{-1}\right)^2\mu^{pq}_{m+1,n} + \left[n\left(\upsilon_{0q}^{-2}-1\right)-n\left(1-\upsilon_{0p}^{-2}\right)\right]\eta^{pq}_{mn} + \left(\upsilon_{0q}-\upsilon_{0q}^{-1}\right)^2\cdot\right.$$
$$\left.\times\sum_{k=1}^{\infty}(2k-n)\eta^{pq}_{m,2k-n} + \frac{2}{d_q}\left(\bar{Z}_{pq}-Z_{pq}\right)\sum_{k=0}^{\infty}(2k+1-n)\eta^{pq}_{m,2k+1-n}\right\} \tag{43}$$

for $n>0$, in accordance with (14),

$$b_{npq} = b_{-n,pq} + n\left(\upsilon_{0q}^2-\upsilon_{0q}^{-2}\right)a_{npq}. \tag{44}$$

Now, we come back to (27) and write

$$\sum_{p=1}^{N} u^s_p(z_p) = u^s_q(z_q) + u^r_q(z_q), \tag{45}$$

where $u^r_q(z_q) = \sum_{p\neq q} u^r_{pq}(z_q)$ has the form (30), (31) with replace φ^r_{pq} to $\varphi^r_q = \sum_{p\neq q}\varphi^r_{pq}$, ψ^r_{pq} to $\psi^r_q = \sum_{p\neq q}\psi^r_{pq}$; also,

$$a_{nq} = \sum_{p\neq q} a_{npq}, \quad b_{nq} = \sum_{p\neq q} b_{npq}. \tag{46}$$

No problems arise with the linear term in (27):

$$u^r(z) = U_q + u^r(z_q), \tag{47}$$

where $U_q = (X_{1q}E_{11} + X_{2q}E_{12}) + \mathrm{i}(X_{1q}E_{12} + X_{2q}E_{22})$ is the constant; $u^r(z_q)$ adds to (46) a few extra terms defined by (19) and thus, the problem has been reduced to that was considered in Section 2.

The resolving set of equations is

$$\begin{aligned}
&\varkappa_0 A_{nq} - \varkappa_q C_{nq} + (\overline{D}_{nq} - 2n\sinh 2\zeta_{0q}\overline{C}_{nq})\upsilon_{0q}^{2n} = -\varkappa_0 a_{nq} + \overline{b}_{-n,q}\upsilon_{0q}^{2n},\\
&\overline{B}_{nq} + \varkappa_q C_{nq}\upsilon_{0q}^{2n} - \overline{D}_{nq} = \varkappa_0 a_{-n,q}\upsilon_{0q}^{2n} - \overline{b}_{nq},\\
&A_{nq} - \lambda_q C_{nq} - \lambda_q(\overline{D}_{nq} - 2n\sinh 2\zeta_{0q}\overline{C}_{nq})\upsilon_{0q}^{2n} = -a_{nq} - \overline{b}_{-n,q}\upsilon_{0q}^{2n},\\
&\overline{B}_{nq} - \lambda_q C_{nq}\upsilon_{0q}^{2n} - \lambda_q\overline{D}_{nq} = -a_{-n,q}\upsilon_{0q}^{2n} - \overline{b}_{nq},\\
&\quad n = 1,2,\ldots, \quad q = 1,2,\ldots,N,
\end{aligned} \tag{48}$$

where $\lambda_q = G_q/G_0$; C_{nq} and D_{nq} are the expansion coefficients of solution in the qth inclusion. To get it in an explicit form for direct solver one needs to substitute (31) and (43) into (46) and then into (48). Alternatively, the simple iterative solving procedure can be applied here: given some initial guess of A_{nq}, B_{nq},C_{nq} and D_{nq} for $1 \leqslant q \leqslant N$, we compute a_{nq} and b_{nq} from (33), (43) and (46), then substitute into the right-hand side of (48) and solve it for the next approximation of unknown coefficients, etc. As our computational practice shows, this procedure works well for a whole range of input parameters excluding the case of nearly touching inclusions where, to provide convergence of numerical algorithm, the initial approximation has to be taken properly.

4. Application to the mechanics of composites

The general solution obtained in the previous section can be applied to study a variety of composite mechanics problem with an accurate account for interactions between the inclusions. With this purpose we will establish a link between the current complex potential approach and another general approach used in micromechanics of composite materials and based on such fundamental notions as Green's function and the Eshelby tensor. Namely, the stress distribution in the medium with the matrix V_0 containing a finite array of homogeneous inclusions V_p with the characteristic functions $H_p(\mathbf{x})$ ($p = 1,\ldots,N$), induced by remote loading $\boldsymbol{\sigma}_\infty(\mathbf{x}) = \boldsymbol{\sigma}_\infty = \text{const.}$ and the disturbances caused by the inclusions is defined from the general integral equation

$$\boldsymbol{\sigma}(\mathbf{x}) = \boldsymbol{\sigma}_\infty + \sum_{i=1}^{N}\int \boldsymbol{\Gamma}(\mathbf{x}-\mathbf{y})\{[\mathbf{M}(\mathbf{y}) - \mathbf{M}_0]\boldsymbol{\sigma}(\mathbf{y}) + \boldsymbol{\beta}(\mathbf{y})\}H_p(\mathbf{y})\,\mathrm{d}\mathbf{y}. \tag{49}$$

Here the constitutive equations

$$\boldsymbol{\sigma}(\mathbf{x}) = \mathbf{L}(\mathbf{x})\boldsymbol{\varepsilon}(\mathbf{x}) + \boldsymbol{\alpha}(\mathbf{x}), \quad \boldsymbol{\varepsilon}(\mathbf{x}) = \mathbf{M}(\mathbf{x})\boldsymbol{\sigma}(\mathbf{x}) + \boldsymbol{\beta}(\mathbf{x}) \tag{50}$$

are assumed where $\mathbf{M} = (\mathbf{L})^{-1}$ and $\mathbf{L}$ are the tensor of compliance and stiffness, $\boldsymbol{\beta}$ and $\boldsymbol{\alpha} \equiv -\mathbf{L}\boldsymbol{\beta}$ are second-order tensors of eigenstrains and eigenstresses, respectively, which are assumed to be vanished in the matrix $v_0 : \boldsymbol{\alpha}(\mathbf{x})$, $\boldsymbol{\beta}(\mathbf{x}) \equiv \mathbf{0}$ ($\mathbf{x} \in V_0$) and $\boldsymbol{\beta}(\mathbf{y}) = \boldsymbol{\beta} = \text{const}$, $\boldsymbol{\alpha}(\mathbf{y}) = \boldsymbol{\alpha} = \text{const}$ ($\mathbf{y} \notin V_0$). The integral operator kernel,

$\boldsymbol{\Gamma}(\mathbf{x}-\mathbf{y}) \equiv -\mathbf{L}_0[\mathbf{I}\delta(\mathbf{x}-\mathbf{y}) + \mathbf{U}(\mathbf{x}-\mathbf{y})\mathbf{L}_0]$, $U_{ijkl}((\mathbf{x}) = [\nabla_q \nabla_l\ G_{ik}(\mathbf{x})]_{(ij)(kl)}$, called the Green stress tensor is defined by the infinite-homogeneous-body Green's function of the Navier equation with an elastic modulus tensor $\mathbf{L}_0 : \nabla\{\mathbf{L}_0[\nabla \otimes \mathbf{G}(\mathbf{x}) + (\nabla \otimes \mathbf{G}(\mathbf{x}))^{\mathrm{T}}]/2\} = -\boldsymbol{\delta}\delta(\mathbf{x})$, vanishing at infinity ($|\mathbf{x}| \to \infty$), $(\cdot)^{\mathrm{T}}$ denotes matrix transposition, and $\delta(\mathbf{x})$ is the Dirac delta function; the subscript pair with parentheses denotes symmetrization on (ij) and (kl).

The comprehensive review of methods used for solution of (49) can be found in the paper by Buryachenko and Pagano (2005). However, in micromechanics of random structure composites only the semi-analytical approximative solutions of (49) based on both the Eshelby tensor $\mathbf{S}_q$ (Eshelby, 1957) and external Eshelby tensor $\mathbf{T}_q^{\varepsilon}(\mathbf{x}-\mathbf{x}_q)$

$$\begin{aligned} &\mathbf{S}_q = -\langle \mathbf{U}(\mathbf{x}-\mathbf{y})\rangle_q \mathbf{L}_0, \quad \mathbf{x},\mathbf{y} \in V_q, \\ &\mathbf{T}_q^{\varepsilon}(\mathbf{x}-\mathbf{x}_q) = \langle \mathbf{U}(\mathbf{x}-\mathbf{y})\rangle_q, \\ &\langle(\cdot)\rangle_q \equiv (\operatorname{mes} v_q)^{-1} \int_{V_q} (\cdot)\mathrm{d}\mathbf{y}, \quad \mathbf{x} \notin V_q, \end{aligned} \tag{51}$$

are usually explored. The tensor $\mathbf{T}_{pq}^{\varepsilon}(\mathbf{x}_p-\mathbf{x}_q) = \langle \mathbf{T}_q^{\varepsilon}(\mathbf{y}-\mathbf{x}_q)\rangle_p$, initially introduced by Willis and Acton (1976) for the spherical identical inclusions (see also numerous references in Buryachenko, 2001), plays a key role in deriving the second-order approximation of effective, or macroscopic, elastic moduli of composite. In the case of a stress analysis of composite materials, it is more convenient to use the following tensors expressed in terms of ones introduced earlier (51):

$$\begin{aligned} &\mathbf{Q}_q = \mathbf{I} - \mathbf{L}_0\mathbf{S}_q, \\ &\mathbf{T}_q^{\sigma}(\mathbf{x}-\mathbf{x}_p) = -\mathbf{L}_0\mathbf{T}_q^{\varepsilon}(\mathbf{x}-\mathbf{x}_p)\mathbf{L}_0, \\ &\mathbf{T}_{pq}^{\sigma}(\mathbf{x}_p-\mathbf{x}_q) = -\mathbf{L}_0\mathbf{T}_{pq}^{\varepsilon}(\mathbf{x}_p-\mathbf{x}_q)\mathbf{L}_0. \end{aligned} \tag{52}$$

For representation of the tensors (52) in the terms of the approach developed in the previous sections, we, at first, will present them in the forms of particular solutions of (49). Namely, for a single homogeneous elliptical inclusion V_q with the matrix elastic properties ($\mathbf{L}_q(\mathbf{x}) \equiv \mathbf{L}_0 = \text{const.}$, $\boldsymbol{\beta}(\mathbf{x}) = \boldsymbol{\beta} = \text{const.} \neq \mathbf{0}$, $\mathbf{x} \in V_q$ and $\boldsymbol{\beta}(\mathbf{x}) \equiv \mathbf{0}$, $\mathbf{x} \notin V_q$)

$$\begin{aligned} &\boldsymbol{\sigma}(\mathbf{x}) = \mathbf{Q}_q\boldsymbol{\beta} \quad \text{for } \mathbf{x} \in V_q, \\ &\boldsymbol{\sigma}(\mathbf{x}) = \mathbf{T}_q^{\sigma}(\mathbf{x}-\mathbf{x}_q)\boldsymbol{\beta} \quad \text{for } \mathbf{x} \notin V_q. \end{aligned} \tag{53}$$

The estimation of the tensors $\mathbf{Q}_q$, $\mathbf{T}_q^{\sigma}(\mathbf{x}-\mathbf{x}_q)$, and $\mathbf{T}_{pq}^{\sigma}(\mathbf{x}_p-\mathbf{x}_q)$ is a particular problem of the transformation field analysis by Dvorak and Benveniste (1992) which can be realized by the different methods, for example by the proposed one. Indeed, let the inclusion be subjected to the eigenstrain $\boldsymbol{\beta}(\mathbf{x}) \equiv \text{const.}$ ($\mathbf{x} \in V_q$) with a single non-zero component $\beta_k = 1$ ($k = 1, 2, 3$), otherwise $\beta_l \equiv 0$ ($l = 1, 2, 3$; $l \neq k$). Here and below, we adopt short, or vectorial, notation: so, $\boldsymbol{\sigma} = (\sigma_{11}, \sigma_{22}, \sigma_{12})^{\mathrm{T}}$, $\boldsymbol{\beta} = (\beta_{11}, \beta_{22}, \beta_{12})^{\mathrm{T}}$, etc. Then, we obtain the explicit representation of the tensors $\mathbf{Q}_p$, $\mathbf{T}_q^{\sigma}$ and $\mathbf{T}_{pq}^{\sigma}$ in terms of the known stress fields $\boldsymbol{\sigma}(\mathbf{x})$ both inside and outside the inclusion V_q:

$$\begin{aligned} &\mathbf{Q}_{q|kj}(\mathbf{x}) = \boldsymbol{\sigma}_j(\mathbf{x}), \quad \mathbf{x} \in V_q, \\ &\mathbf{T}_{q|kj}^{\sigma}(\mathbf{x}-\mathbf{x}_q) = \boldsymbol{\sigma}_j(\mathbf{x}), \quad \mathbf{x} \notin V_q, \\ &\mathbf{T}_{pq|kj}^{\sigma}(\mathbf{x}_p-\mathbf{x}_q) = \langle \boldsymbol{\sigma}_j(\mathbf{y})\rangle_p, \quad \mathbf{y} \in V_p. \end{aligned} \tag{54}$$

In the case of elliptic inclusion shape, the solution obtained in Section 3 can be readily used to evaluate stress field in and around pre-stressed inclusion, and, hence, the tensors $\mathbf{Q}_p$, $\mathbf{T}_q^{\sigma}(\mathbf{x}-\mathbf{x}_q)$, and $\mathbf{T}_{pq}^{\sigma}(\mathbf{x}_p-\mathbf{x}_q)$. The only difference is the second condition in (26) which takes the form

$$[[\boldsymbol{\sigma}\cdot\mathbf{n}]]_{\zeta=\zeta_{0q}}=\boldsymbol{\alpha}\cdot\mathbf{n}\quad\text{or, equivalently,}\quad[[\boldsymbol{\varepsilon}\cdot\mathbf{n}]]_{\zeta=\zeta_{0q}}=\boldsymbol{\beta}\cdot\mathbf{n}. \tag{55}$$

Since the material is homogeneous and $\boldsymbol{\beta}_q$ is non-zero only in one inclusion, with $p=q$, its solution involves only the first harmonics in (8) and (9) and leads to the resolving system quite similar in form to (22). After simple algebra one obtains

$$\begin{aligned}
A_{1q}&=-\frac{d_q\left(\upsilon_{0q}^2-\upsilon_{0q}^{-2}\right)}{4(\varkappa+1)}I_2,\\
B_{1q}&=\frac{d_q\left(\upsilon_{0q}^2-\upsilon_{0q}^{-2}\right)}{4(\varkappa+1)}\left[(1-\varkappa)I_1-I_2\upsilon_{0q}^{-2}\right],\\
C_{1q}&=\frac{d_q}{4(\varkappa+1)}\left(I_1+I_2\upsilon_{0q}^{-2}\right),\\
D_{1q}&=\frac{d_q}{4(\varkappa+1)}\left\{\left[\upsilon_{0q}^2+(\varkappa-1)\upsilon_{0q}^{-2}\right]I_1+\varkappa\overline{I}_2+\left(\upsilon_{0q}^2-\upsilon_{0q}^{-2}\right)I_2\upsilon_{0q}^{-2}\right\},
\end{aligned} \tag{56}$$

where

$$I_1=\frac{2}{(\varkappa-1)}(\beta_{11}+\beta_{22})\quad\text{and}\quad I_2=\beta_{22}-\beta_{11}-2\mathrm{i}\beta_{12}. \tag{57}$$

With A_{1q}, B_{1q}, C_{1q} and D_{1q} determined from (56) and (57), the stress in any point in and around the prestressed inclusion can be evaluated. Substitution of (56) into (8) and (9) and then into (4) followed by comparison with (53) gives us an explicit expression of the tensors $\mathbf{Q}_q$ and $\mathbf{T}_q^{\sigma}$ matching perfectly the analogous results reported elsewhere (e.g., Mura, 1982).

To evaluate $\mathbf{T}_{pq}^{\sigma}$, we derive also the formula for an average stress in the inclusion $\langle\boldsymbol{\sigma}\rangle_p$ assuming $\boldsymbol{\beta}(\mathbf{x})\equiv\mathbf{0}$ ($\mathbf{x}\in V_p$). We rewrite (50) as

$$\boldsymbol{\sigma}_p=\mathbf{L}_p\frac{1}{2}\left[\nabla\mathbf{u}^{(p)}+(\nabla\mathbf{u}^{(p)})^{\mathrm{T}}\right] \tag{58}$$

and substitute it in the representation for $\langle\boldsymbol{\sigma}\rangle_p$ and apply the Gauss theorem to reduce the integral in (51) to that along the boundary S_p of inclusion:

$$\left\langle\boldsymbol{\sigma}_p\right\rangle_p=\frac{1}{2}(\operatorname{mes}v_p)^{-1}\mathbf{L}_p\int_{S_p}(\mathbf{n}\mathbf{u}^{(p)}+\mathbf{u}^{(p)}\mathbf{n})\,\mathrm{d}s. \tag{59}$$

In (59) $\mathbf{n}$ is the outward unit vector normal to the boundary S_p; in the case of the ellipse, $n=n_1+\mathrm{i}n_2=\omega'(\xi_p)/|\omega'(\xi_p)|$. Note also that $\zeta_p=\zeta_{0p}$ at S_p and, in fact, integration in (59) reduces to integration over $0<\eta_p\leqslant 2\pi$. It is rather straightforward to show that only the terms in $u^{(p)}$ series expansion containing the first Fourier harmonics in η give non-zero contribution to (59). After some algebra we come to the following formulas:

$$\begin{aligned}
\langle\sigma_{11}\rangle_p+\langle\sigma_{22}\rangle_p&=\frac{16G_0}{d_p}\operatorname{Re}C_{-1,p},\\
\langle\sigma_{22}\rangle_p-\langle\sigma_{11}\rangle_p+2\mathrm{i}\langle\sigma_{12}\rangle_p&=\frac{8G_0}{d_p}\left(D_{-1,p}-C_{-1,p}\upsilon_{0p}^{-2}\right).
\end{aligned} \tag{60}$$

Noteworthy, this result is valid for an arbitrary, not necessarily uniform, stress field.

According to (54), integration in (60) is made over the area of the pth inclusion, $p\neq q$. Since $\mathbf{L}_q=\mathbf{L}_0$ and $\boldsymbol{\beta}_q\not\equiv 0$, the stress in this inclusion is nothing more than a disturbance field caused by $\boldsymbol{\beta}$ in a vicinity of $z=Z_p$. Thus, we have $C_{np}=a_{nqp}$ and $D_{np}=b_{nqp}$; then, from (60),

$$\langle\sigma_{11}\rangle_p + \langle\sigma_{22}\rangle_p = \frac{16G}{d_p}\mathrm{Re}\, a_{-1,qp},$$
$$\langle\sigma_{22}\rangle_p - \langle\sigma_{11}\rangle_p + 2\mathrm{i}\langle\sigma_{12}\rangle_p = \frac{8G}{d_p}\left(b_{-1,qp} - a_{-1,qp}\upsilon_{0q}^{-2}\right). \tag{61}$$

In turn, the coefficients a_{nqp} and b_{nqp} can be expressed in terms of unknowns A_{nq} and B_{nq} using the formulas (33) and (43). In our specific case,

$$a_{-1,qp} = A_{1q}\eta_{11}^{qp}, \quad b_{-1,qp} = A_{1q}\gamma_{11}^{qp} + B_{1q}\eta_{11}^{qp}. \tag{62}$$

The last remaining step is substitution of (56) into (62) and then into (61), from where an explicit form of $\mathbf{T}_{pq}^{\sigma}$ tensor can be easily recovered by comparison with (54).

5. Numerical study

The series solution derived above is an accurate, asymptotically exact one. This means that to get exact values, one has to solve a whole infinite set of linear equations. In practice, we solve it by applying the reduction method which means that we retain in (48) only a certain *finite* number $n_{\max}$ of equations and unknowns. Based on asymptotic analysis of the linear set (48), it can be proven rigorously (e.g., Kantorovich and Krylov, 1964) that approximate solution obtained in this way converges to an exact one as $n_{\max} \to \infty$. Thus, any desirable accuracy can be achieved by proper choice of $n_{\max}$. So, for the well-separated inclusions (dilute composite case), even $n_{\max} = 1$ provides reasonably good approximation. The smaller the distance between the inclusions (more precisely, closest distance between their boundaries), the higher is order of Fourier harmonics which must be retained in the numerical solution to ensure appropriate accuracy of computations. It is hard to believe that there exists a general rule and, probably, the best way is to find $n_{\max}$ from a series of numerical experiments for each specific problem. Some idea of convergence rate as a function of distance Z_{12} can be drawn from Table 1, where the normalized stress $\sigma_{22}(l_1 + 0\mathrm{i})/S_{22}$ values are given. In the problem considered here, the centers of two identical elliptic holes ($\lambda_1 = \lambda_2 = 0$) with aspect ratios $e_1 = e_2 = 0.3$ in the plane with $\nu_0 = 0.3$ are placed on the Ox_1 axis (see Fig. 1) and the far field is uniaxial tension in the x_2 direction. One-particle solution ($Z_{12} = \infty$) gives an exact answer $\sigma_{22}(l_1 + 0\mathrm{i}) = (1 + 2/e_1)S_{22} = 7\frac{2}{3}S_{22}$; for a finite Z_{12}, the calculated σ_{22} values depend on $n_{\max}$.

As seen from the table, for $Z_{12} = 5l_1$ already $n_{\max} = 5$ provides four-digit accuracy of stress evaluation at the point $z = l_1 + 0\mathrm{i}$ where the stress peak value (and, expectably, lowest convergence rate) is observed. At the same time, for nearly touching holes ($Z_{12} = 2.05l_1$) as many as 25 harmonics are required to get a prac-

Table 1
Convergence rate of $\sigma_{22}(l_1 + 0\mathrm{i})/S_{22}$ as a function of Z_{12}/l_1

$n_{\max}$	$Z_{12} = 5l_1$	$Z_{12} = 3l_1$	$Z_{12} = 2.5l_1$	$Z_{12} = 2.1l_1$	$Z_{12} = 2.05l_1$
1	7.802	8.142	8.513	9.539	9.875
3	7.826	8.340	9.098	12.73	14.70
5	7.824	8.340	9.144	14.14	17.67
7	7.824	8.338	9.139	14.75	18.38
9	7.824	8.337	9.135	15.02	20.40
11	7.824	8.337	9.134	15.16	21.02
13	7.824	8.337	9.133	15.22	21.40
15	7.824	8.337	9.133	15.25	21.63
...	...	...	...	...	...
25	7.824	8.337	9.133	15.28	21.99
FEM	7.82	8.34	9.13	15.29	22.03

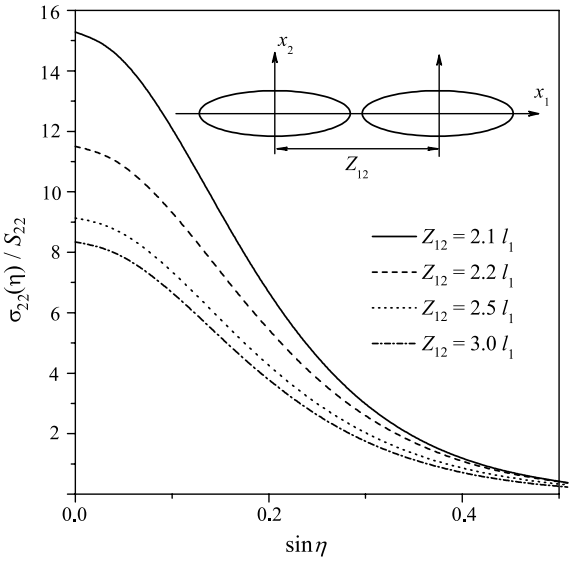

Fig. 1. Stress σ_{22} variation along the first hole surface due to uniaxial tension $S_{22} = 1$ of a plane with two holes as a function of distance Z_{12} between them.

tically convergent solution: deviation from the accurate data obtained by the finite element method (last line of Table 1) does not exceed 0.2%. Based on this observation, the value $n_{\max} = 25$ is adopted for all subsequent calculations.

The problem under study has a number of parameters and its exhaustive parametric study is the subject of a separate paper. In what follows, we restrict ourselves to the two-inclusion problem and show the way and extent to which stress concentration on elliptic inclusions is affected by their position, shape, elastic properties and loading type. So, stress σ_{22} variation along the first hole boundary due to uniaxial tension $S_{22} = 1$ of a plane with two identical holes with aspect ratio $e_2 = 0.3$ as a function of relative distance Z_{12}/l_1 between them is shown in Fig. 1. The σ_{22} stress reaches maximum at $\eta_1 = 0$, i.e. at the point nearest to the next hole and considerable growth of $\max\sigma_{22}$ is observed as the holes are drawn together. At the same time, σ_{22} on the opposite side of the hole ($\eta_1 = \pi$) does not vary much from that for a single hole.

Curves in Fig. 2 demonstrate the effect on σ_{11} variation along the interface of the particle–particle and particle–hole interactions. Here, the far load is $S_{11} = 1$; curves 1–4 are calculated for $\lambda_1 = \lambda_2 = 100$, $\nu_1 = \nu_2 = \nu_0 = 0.3$ (two hard inclusions with $e = 0.3$) whereas curves 5–8 are obtained for $\lambda_1 = 100$, $\lambda_2 = 0$ (hard inclusion and hole). The relative distance Z_{12}/l_1 is equal to 3.0 (curves 1 and 5), 2.5 (curves 2 and 6), 2.2 (curves 3 and 7) and 2.1 (curves 4 and 7). It is seen from Fig. 2 that in the case of two hard inclusions considerable growth of $\max\sigma_{11}$ is observed. On the contrary, the presence of an adjacent hole expectedly results in σ_{11} stress relaxation well below the value we have on a single inclusion.

In Fig. 3, σ_{11} variation is shown for varying aspect ratios and fixed relative position of elliptic fibers, $Z_{12} = 2.1l_1$. Calculations for $0.5 < e < 1$ do not detect a substantial effect on stress concentration of the aspect ratio. However, for e of order 0.3 and less, the peak stress grows rapidly and in the limit $e \to 0$, when elliptic inhomogeneity degenerates into the plane crack of rigid line inclusion, it may become infinitely large, see (23). It was already discussed that the method exposed provides an accurate solution for arbitrary (including $e = 0$) aspect ratio, and no numerical difficulties arise due to this small parameter. A numerical example showing inclusion–crack interaction will be given at the end of this section.

The effect on stress distribution of the relative position of the inclusions is clearly seen from Fig. 4, where curve 1 corresponds to $Z_{12} = 2.1l_1$ (centers of holes lie on the Ox_1), curve 2 shows σ_{11} for intermediate

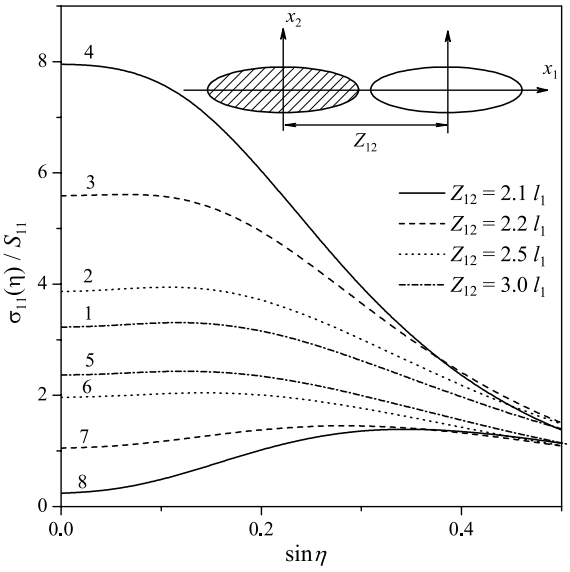

Fig. 2. Stress σ_{11} variation along the first inclusion surface due to uniaxial tension $S_{11} = 1$ of a plane with two inclusions as a function of distance Z_{12} between them.

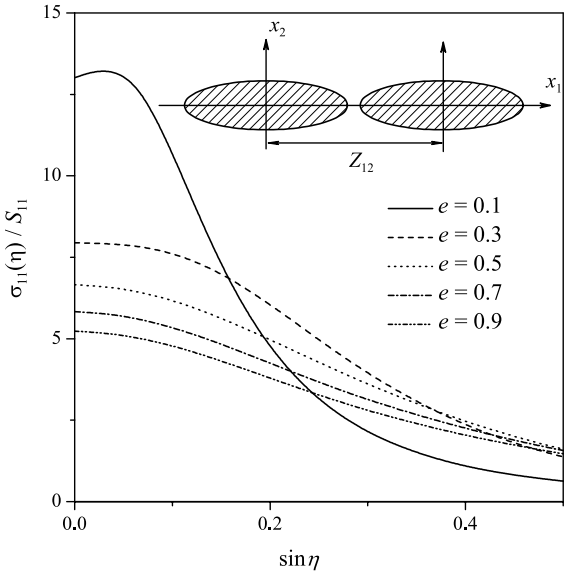

Fig. 3. Stress σ_{11} variation along the first inclusion surface due to uniaxial tension $S_{11} = 1$ of a plane with two elliptic inclusions as a function of their aspect ratio e, $Z_{12} = 2.1l_1 + 0\mathrm{i}$.

position $Z_{12} = l_1 + 2l_2\mathrm{i}$ and curve 3 is calculated for $Z_{12} = 2.1l_2\mathrm{i}$ (one ellipse above another); $e_1 = e_2 = 0.3$ and $S_{11} = 1$. In contrast to the first case where σ_{11} in a vicinity of the point $z_1 = l_1 + 0\mathrm{i}$ is more than two times higher than that on a single inclusion, in the case of the two elliptic inclusions arranged in the x_2 direction $\max\sigma_{11}$ is well below that value. This so-called "shielding" effect is observed not only for the peak stress but also for the averaged stress in the inclusion (see Fig. 6).

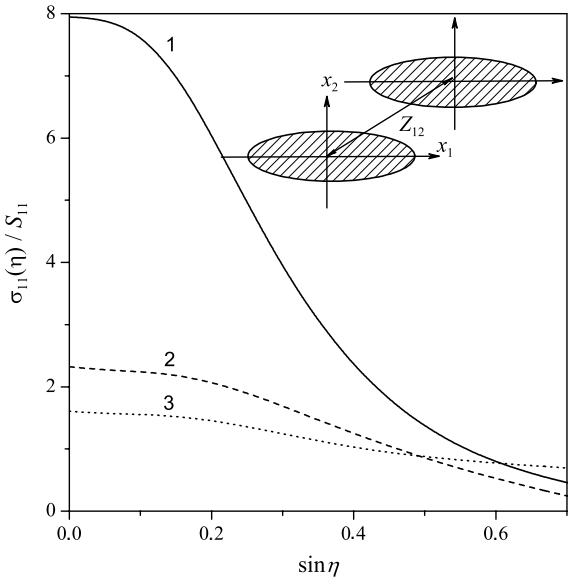

Fig. 4. Stress σ_{11} variation along the first inclusion surface due to uniaxial tension $S_{11} = 1$ of a plane with two elliptic inclusions as a function of relative position: line 1 – $Z_{12} = 2.1l_1 + i0$; line 2 – $Z_{12} = l_1 + 2l_2 i$; line 3 – $Z_{12} = 0 + 2.1l_2 i$.

The above presented data are summarized in the next two tables, where an interface stress concentration factor defined as $K_{ijkl} = \max_\eta \sigma_{ij}(\eta)/S_{kl}$, with σ_{ij} calculated for the uniform far stress field $S_{nm} = \delta_{nk}\delta_{ml}$ is given. So, $K_{ijkl}(\infty)$ represents stress concentration on a single inclusion being a function of its shape and elastic properties. To evaluate the particle–particle interaction effect on the interface stress, we.introduce the normalized stress concentration factor (NSCF) as $K_{ijkl}(Z_{12})/K_{ijkl}(\infty)$. The calculated NSCF $K_{2222}(Z_{12})/K_{2222}(\infty)$ values for two elliptic holes are shown in Table 2 whereas Table 3 contains the values

Table 2
Normalized stress concentration factor $K_{2222}(Z_{12})/K_{2222}(\infty)$ as a function of Z_{12}/l_1 and e for two identical elliptic holes: $\lambda_1 = \lambda_2 = 0$; $\nu_0 = 0.3$

Z_{12}/l_1	$e = 0.1$	$e = 0.3$	$e = 0.5$	$e = 0.7$	$e = 0.9$
3.0	1.106	1.087	1.073	1.069	1.079
2.5	1.215	1.191	1.201	1.246	1.316
2.2	1.467	1.500	1.657	1.832	1.976
2.1	1.772	1.993	2.352	2.629	2.822
2.05	2.234	2.868	3.468	3.848	4.078

Table 3
Normalized stress concentration factor $K_{1111}(Z_{12})/K_{1111}(\infty)$ as a function of Z_{12}/l_1 and e for two identical hard elliptic inclusions: $\lambda_1 = \lambda_2 = 100$; $\nu_0 = \nu_1 = \nu_2 = 0.3$

Z_{12}/l_1	$e = 0.1$	$e = 0.3$	$e = 0.5$	$e = 0.7$	$e = 0.9$
3.0	1.132	1.193	1.258	1.319	1.380
2.5	1.280	1.432	1.572	1.689	1.777
2.2	1.652	2.069	2.366	2.528	2.606
2.1	2.115	2.951	3.348	3.467	3.474
2.05	2.969	4.324	4.695	4.680	4.570

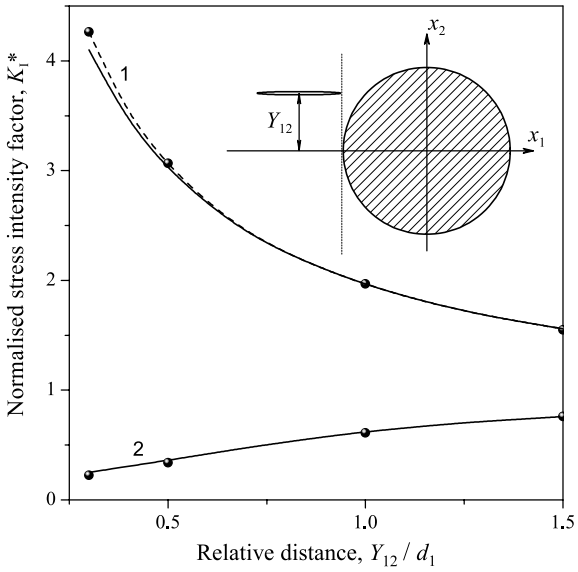

Fig. 5. Normal opening mode SIF $K_1/\sqrt{\pi d_1/S_{22}}$ of a crack nearby circular inclusion or hole as a function of relative position $Z_{12}/l_1 = 3 + Y_{12}/l_1$: line $1 - \lambda_2 = 0$; line $2 - \lambda_2 = 23$; solid points represent the data by Erdogan et al. (1974).

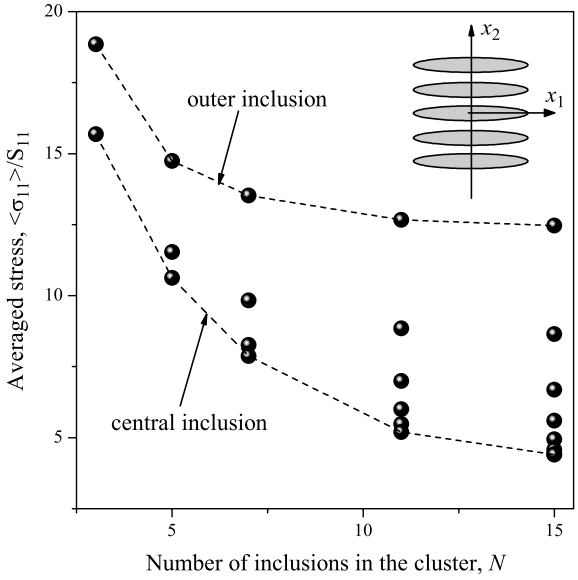

Fig. 6. Average stress $\langle\sigma_{11}\rangle$ in the inclusions due to uniaxial tension $S_{11} = 1$ of a plane with a finite cluster of thin hard inclusions.

$K_{1111}(Z_{12})/K_{1111}(\infty)$ for two hard elliptic inclusions as a function of Z_{12}/l_1 and e. In both cases considered, the tendency is quite similar: NSCF is growing up as inhomogeneities move toward each other. Also, for Z_{12} being fixed the maximum NSCF values are observed on circular holes and near-to-circular hard inclusions although corresponding absolute stress values for $e = 0.1$ are 3 to 4 times higher than those for $e = 0.9$.

In the next example we consider, the inclusions differ in size, shape and properties. Specifically, we put $e_1 = 0$ and $\lambda_1 = 0$ to degenerate the first inclusion into a crack; the second inclusion is taken circular ($e_2 = 1$), with radius $R_2 = 2d_1$. In Fig. 5, the dimensionless stress intensity factor $K_I^* = K_I/\sqrt{\pi d_1}$ calculated according to (24) for $S_{22} = 1$ is shown as a function of relative distance, Y_{12}/l_1. Curves 1 and 2 correspond to $\lambda_2 = 0$ and $\lambda_2 = 23$, respectively; $\nu_0 = 0.35$ and $\nu_2 = 0.3$. The solid points represent the data obtained by Erdogan et al. (1974) who used the method of singular integral equations. Expectedly, SIF decreases as the crack approaches hard inclusion and grows rapidly in a vicinity of the hole. Close correlation between our results and Erdogan's data can serve as yet another validation of the theory developed and numerical results presented in the paper. A slight discrepancy between the compared results for $Y_{12}/l_1 = 0.3$ means that the value $n_{\max} = 25$ adopted by us for numerical study is not sufficient. Indeed, in the last case a gap between the crack tip and boundary of the hole is about $0.02l_1$ only. For such a geometry, the convergence rate of series (24) is rather slow (see Table 1) and hence additional harmonics must be taken into account in the practical solution to ensure sufficient accuracy of numerical results. Retaining in solution the harmonics up to $n_{\max} = 40$ (the dotted line in Fig. 5) gives $K_I^* = 4.26$ which differs from the value reported by Erdogan et al. (1974) by less than 0.1%.

To complete this section, we give one application of the theory developed to the specific problem of composite mechanics studied by Sheng et al. (2004) where a polymer nanocomposite of clustered structure was considered. There, an isolated cluster was idealized as a multi-layer stack containing N silicate plates with uniform interlayer spacing. The experimentally observed plate thickness was roughly 1nm, the layer spacing ranged from 2 to over 5 nm, and the number of plates per cluster varied from 1 to 50. In our model, the silicate nanolayers are approximated by aligned ellipses with aspect ratio $e = 0.01$, Young's modulus $E_1 = 300$ GPa and Poisson's ratio $\nu_1 = 0.4$ embedded into *Epox*862 matrix with $E_0 = 3.01$ GPa and $\nu_0 = 0.41$ (see Tandon et al., 2002; Sheng et al., 2004). The number of inclusions varied from 1 to 15, and their position is given by $Z_p = 0 + 4(p-1)l_2\mathrm{i}$, $p = 1, 2, \ldots, N$. In Fig. 6, the averaged stress concentration factor $\langle\sigma_{11}\rangle/S_{11}$ calculated from (61) for each inclusion in the cluster is shown by the solid points. As computations show, for a single inclusion $\langle\sigma_{11}\rangle/S_{11} = 34.6$; for $N = 15$, it decreases more than two times even for the outer ellipses where the average stress reaches maximum. Also, variation of $\langle\sigma_{11}\rangle/S_{11}$ grows up with the number of inclusions N increased and reaches 300% in the cluster of 15 inclusions while for $N = 5$ stress concentration factor is varying just on 40%. Such a behavior is qualitatively confirmed by 2D finite element analysis by Sheng et al. (2004) of three rectrangular inclusion in the matrix.

6. Conclusions

In the present work, an accurate analytical solution has been developed for a piece-homogeneous elastic plane containing a finite array of elliptic inclusions of arbitrary size, aspect ratio, location and elastic properties. The method developed combines Muskhelishvili's representation of general solution in terms of complex potentials with the superposition principle and newly derived re-expansion formulae to obtain a complete solution of the many-inclusion problem. By exact satisfaction of all the interface boundary conditions, the primary boundary-value problem stated on a complicated multiply connected domain has been reduced to an ordinary, well-posed set of linear algebraic equations. The properly chosen form of potentials provides a remarkably simple form of solution and thus an efficient computational algorithm. The theory developed is rather general and can be applied to solve a variety of composite mechanics problems. The advanced models of composite which involve up to several hundred inclusions and thus provide an accurate account for the microstructure statistics and fiber–fiber interactions can be considered in this way. The numerical examples are given showing high accuracy and numerical efficiency of the method developed and disclosing the way and extent to which the selected structural parameters influence the stress concentration at the matrix–inclusion interface.

Acknowledgment

This work was supported by the European Office of Aerospace Research and Development (EOARD) through STCU Grant # P-110.

Appendix A. Auxiliary theoretical results

A.1. Displacement and traction at the elliptic interface

Let us start with the displacement **u** given by (3). It contains derivative $\varphi'(z) = \mathrm{d}\varphi/\mathrm{d}z$, which can be rewritten as

$$\varphi'(z) = \frac{\mathrm{d}\varphi}{\mathrm{d}\xi}\frac{\mathrm{d}\xi}{\mathrm{d}z} = \frac{\varphi'(\xi)}{\omega'(\xi)}. \tag{A.1}$$

Taking also account of that on the ellipse $\zeta = \zeta_0$

$$(z - \bar{z}) = d\sinh\zeta_0(\mathrm{e}^{\mathrm{i}\eta} - \mathrm{e}^{-\mathrm{i}\eta}), \tag{A.2}$$

we get for the second term in (3)

$$-(z-\bar{z})\overline{\varphi'(z)} = \frac{d\sinh\zeta_0}{\overline{\omega'(\xi)}}(\mathrm{e}^{\mathrm{i}\eta} - \mathrm{e}^{-\mathrm{i}\eta})\sum_n n\overline{A}_n\mathrm{e}^{-n\zeta_0+\mathrm{i}n\eta}. \tag{A.3}$$

On the other hand, the second term in (9) for $\zeta = \zeta_0$ is

$$\psi_1 = \frac{d\sinh\zeta_0}{\omega'(\xi)}\sum_n nA_n(\mathrm{e}^{\mathrm{i}\eta} - \mathrm{e}^{-\mathrm{i}\eta})\mathrm{e}^{-n\zeta_0-\mathrm{i}n\eta}. \tag{A.4}$$

It is clear that these terms cancel each other in (3) and, thus, one obtains

$$u|_{\zeta=\zeta_0} = \varkappa\varphi - \overline{\psi_0} = \sum_n(\varkappa A_n\upsilon^{-n} - \overline{B_n\upsilon^{-n}}). \tag{A.5}$$

Now we proceed with the traction vector T_n in the form (7). Taking account of (A.1) gives us

$$\frac{(\sigma_{\zeta\zeta} - \mathrm{i}\sigma_{\zeta\eta})}{2G} = \frac{\varphi'}{\omega'} + \frac{\overline{\varphi'}}{\overline{\omega'}} - \frac{\omega'}{\overline{\omega'}}\left[(\overline{\omega} - \omega)\frac{\varphi'' - \frac{\omega}{\omega'}\varphi'}{(\omega')^2} - \frac{\varphi'}{\omega'} + \frac{\psi'}{\omega'}\right]. \tag{A.6}$$

Hereinafter, the argument ξ is omitted and differentiation is made with respect to ξ. Next, we re-group it to

$$\frac{(\sigma_{\zeta\zeta} - \mathrm{i}\sigma_{\zeta\eta})}{2G} = \frac{\overline{\varphi'} - \psi_0'}{\overline{\omega'}} + \frac{1}{\omega'\overline{\omega'}}\left[(\omega' + \overline{\omega'})\varphi' + \omega'\psi_1' - (\overline{\omega} - \omega)\left(\varphi'' - \frac{\omega}{\omega'}\varphi'\right)\right]. \tag{A.7}$$

It follows from (A.1)–(A.4) that for $\zeta = \zeta_0$

$$\psi_1 = \frac{(\overline{\omega} - \omega)}{\omega'}\varphi', \tag{A.8}$$

being substituted into (A.7), it gives

$$\frac{(\sigma_{\zeta\zeta} - \mathrm{i}\sigma_{\zeta\eta})}{2G} = \frac{\overline{\varphi'} - \psi_0'}{\overline{\omega'}} + \frac{1}{\omega'\overline{\omega'}}\left[(\omega' + \overline{\omega'})\varphi' - (\overline{\omega} - \omega)\varphi'' + \omega'\psi_1' + \omega\psi_1\right]. \tag{A.9}$$

Now, differentiation of ψ_1 (9) with respect to ξ yields

$$\omega'\psi_1' + \omega\psi_1 = -d\sinh\zeta_0 \sum_n nA_n\left[(n-1)\mathrm{e}^{\mathrm{i}\eta} - (n+1)\mathrm{e}^{-\mathrm{i}\eta}\right]\mathrm{e}^{-n\zeta_0 - \mathrm{i}n\eta}. \tag{A.10}$$

On the other hand, we combine (A.2) with

$$\omega' + \overline{\omega'} = d\sinh\zeta_0(\mathrm{e}^{\mathrm{i}\eta} + \mathrm{e}^{-\mathrm{i}\eta}) \tag{A.11}$$

to prove that

$$(\omega' + \overline{\omega'})\varphi' - (\overline{\omega} - \omega)\varphi'' = d\sinh\zeta_0 \sum_n nA_n\mathrm{e}^{-n\zeta_0 - \mathrm{i}n\eta}\left[n(\mathrm{e}^{\mathrm{i}\eta} - \mathrm{e}^{-\mathrm{i}\eta}) - (\mathrm{e}^{\mathrm{i}\eta} + \mathrm{e}^{-\mathrm{i}\eta})\right] \tag{A.12}$$

is equal to (A.10) with opposite sign. Thus, the whole expression in square brackets in (A.7) is equal to zero and we obtain, by taking conjugate of (A.9),

$$\omega'\left.\frac{T_n}{2G}\right|_{\zeta=\zeta_0} = \varphi' - \overline{\psi_0'} = \sum_n (-n)\left(A_n\upsilon^{-n} - \overline{B_n\upsilon^{-n}}\right). \tag{A.13}$$

A.2. Regularity condition

To prove regularity of the displacement field under condition (14) imposed we show that the separate terms in (3) are the polynomials of variables x_1 and x_2. First, φ can be written as

$$\varphi(z) = C_n(\upsilon^n + \upsilon^{-n}) = 2C_n\cosh[n\,\mathrm{Arccosh}(z/d)], \tag{A.14}$$

we recognize that the hyperbolic cosine standing on the right-hand side of Eq. (A.14) is the nth degree Chebyshev's polynomial of complex variable z/d. It is quite clear that its derivative with respect to $z\varphi'(z)$ as well as the product $(z-\bar{z})\overline{\varphi'}$ satisfies the regularity condition as well.

Next,

$$\psi_0 = D_n\upsilon^{-n} + D_{-n}\upsilon^n = D_{-n}(\upsilon^n + \upsilon^{-n}) + 2nC_n\sinh 2\zeta_0\upsilon^{-n}; \tag{A.15}$$

here, the first term is, likewise (A.14), the polynomial of degree n whereas the second one has the singularity points at $z = \pm d$. However, it is rather straightforward to show that the difference

$$\psi_1 - 2nC_n\sinh 2\zeta_0\upsilon^{-n} = nC_n\frac{\sinh\zeta_0}{\sinh\xi}\left[(\upsilon^{n-1} - \upsilon^{-(n-1)})\upsilon_0 - (\upsilon^{n+1} - \upsilon^{-(n+1)})/\upsilon_0\right] \tag{A.16}$$

is also a polynomial of z: it follows directly from the fact that

$$\frac{\mathrm{d}}{\mathrm{d}z}(\upsilon^n + \upsilon^{-n}) = n\frac{\upsilon^n - \upsilon^{-n}}{d\sinh\xi}. \tag{A.17}$$

Thus, a sum $\psi = \psi_0 + \psi_1$ and, hence, u (3) is regular provided the coefficients C_n and D_n with positive and negative indices satisfy the conditions (14).

Appendix B. Re-expansion formulae for singular complex potentials

Our aim is to re-expand the singular complex potentials $\varphi_p^s = \sum_{n=1}^{\infty} A_{np}\upsilon_p^{-n}$, written in variables of pth local curvilinear coordinate system, into a series $\varphi_{pq}^r = \sum_n a_{npq}\upsilon_q^{-n}$, expressed in the variables of the qth coordinate system. In what follows, we derive the formula

$$\upsilon_p^{-n} = \sum_m \eta_{nm}^{pq}\upsilon_q^{-m}, \quad n = 1, 2, \ldots, \tag{B.1}$$

where $\upsilon_p = \exp\xi_p = z_p/d_p \pm \sqrt{(z_p/d_p)^2 - 1}$, $z_p = z_q + Z_{pq}$ and the expansion coefficients $\eta_{nm}^{pq} = \eta_{nm}(Z_{pq}, d_p, d_q)$ for $p, q = 1, 2, \ldots, N$. In the particular case $d_p = d_q$ and $X_{2p} = X_{2q}$, Meisner and Kouris (1995) expressed η_{nm} as an infinite integral of the modified Bessel functions of first kind product. Here, we obtain an explicit expression of η_{nm}^{pq} by a series of rational functions for the arbitrary position and parameters of coordinate systems.

The most straightforward way[2] is to combine the three following easy-to-derive expansions:

$$\upsilon_p^{-n} = \sum_{k=0}^{\infty} \frac{n}{n+2k} C_{n+2k}^k \left(\frac{d_p}{2z_p}\right)^{n+2k}, \quad |z_p| > d_p, \tag{B.2}$$

$$z_p^{-n} = \sum_{k=0}^{\infty} C_{n+k-1}^k (-1)^k Z_{pq}^{-(n+k)} z_q^k, \quad |z_q| < |Z_{pq}|, \tag{B.3}$$

and

$$\left(\frac{2z_q}{d_q}\right)^n = \sum_{k=0}^{n} C_n^k \upsilon_q^{2k-n}. \tag{B.4}$$

The last formula is finite and has no geometric restrictions. Substituting (B.3) into (B.2) and then (B.4) into the resulting expression gives, after a bit of algebra, the following expression of η_{nm} in (B.1)

$$\eta_{nm}^{pq} = n d_p^n (-1)^m \sum_{l=0}^{\infty} d_q^{2l+m} M_{nml}(d_p, d_q) \frac{(n+m+2l-1)!}{(2Z_{pq})^{n+m+2l}}, \tag{B.5}$$

where

$$M_{nml}(d_p, d_q) = \sum_{k=0}^{l} \frac{(d_p/d_q)^{2k}}{k!(l-k)!(k+n)!(m+l-k)!}. \tag{B.6}$$

Noteworthy, in the case $d_p = d_q$ this expression simplifies to (Kushch, 1996)

$$M_{nml} = \frac{(n+m+l+1)_l}{l!(n+l)!(m+l)!}, \tag{B.7}$$

where $(n)_m$ is Pohgammer's symbol. The obtained expression (B.5) is simple and easy to compute. Note also $\eta_{nm} = \eta_{n,-m}$; it follows directly from the fact that υ_p^{-n} is regular in a vicinity of Z_q, and hence its expansion must comply with the condition (14). However, its principal drawback is the geometric restrictions, narrowing substantially its convergence area. Two of them, namely $|z_p| > d_p$ and $|z_q| < |Z_{pq}|$ came from (B.2) and (B.3), respectively; $|Z_{pq}| > (d_p + d_q)$ is an additional condition providing series convergence in (B.5).

To fix this problem, we rewrite (B.5) in a somewhat different form. Namely, we transform it according to the formula

$$\left(\frac{d_{pq}}{2Z_{pq}}\right)^n = \sum_{k=0}^{\infty} (-1)^k C_{n+k-1}^k \upsilon_{pq}^{-(n+2k)}, \tag{B.8}$$

where $d_{pq} = d_p + d_q$ and $\upsilon_{pq} = Z_{pq}/d_{pq} + \sqrt{(Z_{pq}/d_{pq})^2 - 1}$. After appropriate change of summation order, we come to

[2] This derivation is rather illustrative and does not pretend to be mathematically rigorous. A general and theoretically substantiated scheme of derivation of the type (B.1) expansions was suggested by Ivanov (1968). His rather involved, based on the integral transform technique approach is flawless from a mathematical standpoint. However, in our case the final result coincides with (B.9), obtained by means of standard algebra.

$$\eta_{nm}^{pq} = (-1)^m n \left(\frac{d_p}{d_{pq}}\right)^n \sum_{j=0}^{\infty} \upsilon_{pq}^{-(n+m+2j)} \sum_{l=0}^{j} \frac{(-1)^{j-l}}{(j-l)!} \left(\frac{d_p}{d_{pq}}\right)^{m+2l} M_{nml}(d_p, d_q) \frac{(n+m+l+j-1)!}{(j-l)!}. \tag{B.9}$$

It can be proven that a series (B.1) converges within an ellipse centered in Z_q with inter-foci distance d_{pq} and passing the pole of pth elliptic coordinate system closest to Z_q.

As is easily seen, such a convergence area is quite sufficient to solve for any two non-overlapping ellipses. For well-separated inclusions, both (B.5) and (B.9) give the same numerical value of η_{nm}. Therefore, when we solve numerically for many inclusions, the computational effort-saving strategy is to apply (B.9) to closest neighbors whereas interaction of the rest, more distant inclusions is evaluated using more simple formula (B.5).

Finally, we mention two useful consequences of the formula (B.1). The first of them can be obtained by differentiating both parts of (B.1) with respect to z_q. It gives us

$$\frac{\upsilon_p^{-n}}{\sinh \xi_p} = \frac{d_p}{d_q} \sum_m \frac{m}{n} \eta_{nm}^{pq} \frac{\upsilon_q^{-m}}{\sinh \xi_q}, \tag{B.10}$$

being, in fact, an addition theorem for the alternate set of basic functions (see comments to the Eq. (9)). Another differentiation of (B.1), this time with respect to Z_{pq} results in

$$\frac{\upsilon_p^{-n}}{\sinh \xi_p} = \sum_n \mu_{nm}^{pq} \upsilon_q^{-m}, \tag{B.11}$$

where $\mu_{nm}^{pq} = \frac{d_p}{n} \frac{d}{dZ_{pq}} \eta_{nm}^{pq}$. For μ_{nm} we also have two (general and simplified) expressions obtained by differentiating (B.9) and (B.5), respectively.

References

Buryachenko, V.A., 2001. Multiparticle effective field and related methods in micromechanics of composite materials. Appl. Mech. Rev. 54, 1–47.

Buryachenko, V.A., Kushch,V.I., in press. Effective transverse elastic moduli of composites at non-dilute concentration of a random field of aligned fibers. ZAMP.

Buryachenko, V.A., Pagano, N.J., 2005. The multiscale analysis of multiple interacting inclusions problem: finite number of interacting inclusions. Math. Mech. Solids 10, 25–62.

Bystroem, J., 2003. Influence of the inclusions distribution on the effective properties of heterogeneous media. Composites: Part B 34, 587–592.

Dvorak, G.J., Benveniste, Y., 1992. On transformation strains and uniform fields in multiphase elastic media. Proc. Roy. Soc. London A 437, 291–310.

Erdogan, F., Gupta, G.D., Ratwani, M., 1974. Interaction between a circular inclusion and an arbitrary oriented crack. ASME J. Appl. Mech. 41, 1007–1013.

Eshelby, J.D., 1957. The determination of the elastic field of an ellipsoidal inclusion, and related problems. Proc. Roy. Soc. London A 241, 376–396.

Golovchan ,V.T., Guz, A.N., Kohanenko, Yu., Kushch, V.I., 1993. Mechanics of Composites (in 12 v.). Statics of Materials, vol. 1. Naukova Dumka, Kiev.

Horii, H., Nemat-Nasser, S., 1985. Elastic field of interacting inhomogeneities. Int. J. Solids Structures 21, 731–745.

Ivanov, E.A., 1968. Diffraction of Electromagnetic Fields on Two Bodies. Nauka i Technika, Minsk.

Kaloerov, S.A., Goryanskaya, E.S., 1995. Two-dimensional stress state of multiply-connected anisotropic solid with holes and cracks. Theor. Appl. Mech. 25, 45–56.

Kantorovich, L.V., Krylov, V.I., 1964. Approximate Methods of Higher Analysis. Wiley, New York.

Kosmodamiansky, A.S., 1972. Stress Distribution in the Isotropic Multiply-connected Solids. University Publ., Donetsk.

Kushch, V.I., 1996. Elastic equilibrium of a medium containing finite number of aligned spheroidal inclusions. Int. J. Solids Structures 33, 1175–1189.

Lu, S.-Y., Kim, S., 1990. Effective thermal conductivity of composites containing spheroidal inclusions. AIChe J. 36, 927–938.

Meisner, M.J., Kouris, D.A., 1995. Interaction of two elliptic inclusions. Int. J. Solids Structures 32, 451–466.
Mura, T., 1982. Micromechanics of Defects in Solids. Martinus Nijhoff, Netherlands.
Muskhelishvili, N.I., 1953. Some Basic Problems of the Mathematical Theory of Elasticity. Groningen P. Noordhoff.
Noda, N.-A., Matsumo, T., 1998. Singular integral equation method for interaction between elliptic inclusions. ASME J. Appl. Mech. 65, 310–319.
Sheng, N., Boyce, M.C., Parks, D.M., Rutledge, G.C., Abes, J.I., Cohen, R.E., 2004. Multiscale micromechanical modeling of polymer/clay nanocomposites and the effective clay particle. Polymer 45, 487–506.
Stevenson, A.C., 1942. On the equilibrium of plates. Philos. Mag. 33 (Ser.7), 639–661.
Tandon, G.P., Kim, R.Y., Rice, B.P., 2002. Influence of vapor-grown carbon nanocomposites on thermomechanical properties of graphite–epoxy composites. In: Proc. American Society for Composites 17th Technical Conference. Purdue University, West Lafayette, Indiana, Paper 2039.
Willis, J.R., Acton, J.R., 1976. The overall elastic moduli of a dilute suspension of spheres. Quart. J. Mech. Appl. Math. 29, 163–177.